

Constraining the emergent dark energy models with observational data at intermediate redshift

GuangZhen Wang¹, Xiaolei Li², Nan Liang^{1,3*}

¹*Key Laboratory of Information and Computing Science Guizhou Province (School of Cyber Science and Technology), Guizhou Normal University, Guiyang, Guizhou 550025, China.

²College of Physics, Hebei Normal University, Shijiazhuang, Heibei 050024, China.

³Joint Center for FAST Sciences Guizhou Normal University Node, Guiyang, Guizhou 550025, China.

*Corresponding author(s). E-mail(s): liangn@bnu.edu.cn;

Contributing authors: guangzhenwang@gznu.edu.cn; lixiaolei@hebtu.edu.cn;

Abstract

In this work, we investigate the phenomenologically emergent dark energy (PEDE) model and its generalized form, namely the generalized emergent dark energy (GEDE) model, which introduces a free parameter Δ that can discriminate between the Λ CDM model and the PEDE model. Fitting the emergent dark energy (EDE) models with the observational datasets including the cosmology-independent gamma-ray bursts (GRBs) and the observational Hubble data (OHD) at intermediate redshift, we find a large value of H_0 which is close to the results of local measurement of H_0 from the SH0ES Collaboration in both EDE models. In order to refine our analysis and tighten the constraints on cosmological parameters, we combine mid-redshift observations GRBs and OHD with baryon acoustic oscillations (BAOs). Finally, we constrain DE models by using the simultaneous fitting method, in which the parameters of DE models and the relation parameters of GRBs are fitted simultaneously. Our results suggest that PEDE and GEDE models can be possible alternative to the standard cosmological model, pending further theoretical explorations and observational verifications.

Keywords: Hubble constant, Dark energy, Gamma-ray bursts

1 Introduction

One of the crucial cosmological discoveries was the late-time accelerated expansion of the universe (Riess et al. 1998; Perlmutter et al. 1999), a phenomenon that remains mysterious within the current cosmological framework. To provide a plausible explanation, the concept of an exotic cosmic component dark energy (DE) which produces negative pressure with a negative equation

of state was introduced. The late-time accelerated expansion of the universe can be modeled by the Λ CDM model, which combining the simplest assumption for dark energy: the cosmological constant Λ with an equation of state (EoS) parameter $w = -1$ and the cold dark matter (CDM) component. The standard Λ CDM model has successfully described numerous cosmological observations, including Type Ia supernovae (SNe Ia) (Riess et al. 2007; Scolnic et al. 2018),

baryon acoustic oscillations (BAOs) (Beutler et al. 2011; Ross et al. 2015; Alam et al. 2017; Zhao et al. 2019; Alam et al. 2021), and the cosmic microwave background (CMB) (Ichiki and Nagata 2009; Komatsu et al. 2011; Planck Collaboration et al. 2016, 2020). The measurement of the Hubble constant (H_0) has revealed the current accelerated expansion of the Universe (Freedman and Madore 2010). The H_0 tension is one of the major issues in modern cosmology in which the measurements discrepancy between the local measurement of H_0 by the *Supernova H_0 for the Equation of State* (SH0ES) collaboration (Riess et al. 2016, 2018, 2019, 2022b,a) and the early Universe using Planck CMB observations assuming the Λ CDM model (Planck Collaboration et al. 2016, 2020) can reach at 5.3σ . At a $1\text{-}\sigma$ confidence level, SH0ES measurement of the distance ladder calibrated by Cepheids yields $H_0 = 73.01 \pm 0.99 \text{ km s}^{-1} \text{ Mpc}^{-1}$ (Riess et al. 2022a); whereas the Planck collaboration which uses temperature and polarization anisotropies in the CMB obtain $H_0 = 67.27 \pm 0.6 \text{ km s}^{-1} \text{ Mpc}^{-1}$ (Planck Collaboration et al. 2020). The H_0 tension implies that either there are considerable but not accounted for systematic errors in observations, or modifications to the standard Λ CDM model might be considered, see (O’Dea et al. 2007; Bunn 2007; Di Valentino et al. 2021) and reference therein.

With a motivation of alleviating the H_0 tension, Li and Shafieloo (2019) proposed a new dark energy model called the Phenomenologically Emergent Dark Energy (PEDE) model as a potential alternate to the Λ CDM model. The model effectively replaces the cosmological constant with a hyperbolic tangent function of redshift which causes the DE to emerge as a function of the cosmic time at later times. Pan et al. (2020) found that the tension on H_0 is clearly alleviated for the PEDE model in a six parameter space similar to the spatially flat Λ CDM model with the combined datasets. Koo et al. (2020) used a non-parametric iterative smoothing method on the Joint Light-curve Analysis (JLA) SNe Ia data to show that the PEDE model are consistent with those of the standard model. Yang et al. (2023) considered the effects of adding curvature in the PEDE model with the Planck 2018 CMB temperature and polarization data, BAO and Pantheon sample (Scolnic et al. 2018) which contains 1048

SNe Ia data. Liu et al. (2022a) used a newly compiled sample the ultra-compact structure in radio quasars and strong gravitational lensing systems with quasars to constrain the spatially flat and non-flat PEDE model.

Later on, Li and Shafieloo (2020) proposed the Generalized Emergent Dark Energy (GEDE) model with extra parameters to describe the properties of dark energy evolution: the free parameter Δ describe the evolution slope of dark energy density, and the transition redshift z_t which identifies where dark energy density equals matter density is not a free parameter. The GEDE model has the flexibility to include both the Λ CDM model and the PEDE model as two of its special limits. Motta et al. (2021) briefly summarize the characteristics of a list of dark energy models including the PEDE and GEDE models with the joint cosmological samples.

There is an interesting idea for the H_0 tension for H_0 with a redshift evolving of observational data. Recently, Dainotti et al. (2021) find a slowly decreasing trend of H_0 value with a function mimicking the redshift evolution. The local distance ladder of SN Ia calibrated by Cepheids can reach at $z < 0.01$, while the CMB data is near $z \sim 1000$. Therefore, cosmological data in the mid-redshift region between the local distance ladder and CMB might offer important insights into the origins of the H_0 tension. Gamma-ray bursts (GRBs) are extremely powerful and bright sources that are observed up to very high redshifts, reaching at $z = 8.2$ (Tanvir et al. 2009) and $z = 9.4$ (Cucchiara et al. 2011). Therefore, GRBs can be used to probe the high-redshift universe beyond SNe Ia. Due to the lack of a low-redshift sample, a fiducial cosmological model should be assumed for calibrating the GRB luminosity relations in the early cosmological studies (Dai et al. 2004). The so-called circularity problem (Ghirlanda et al. 2006) will be encountered. For the purpose to avoid the circularity problem, Liang et al. (2008) proposed a cosmological model-independent method to calibrate the luminosity relations of GRBs by using the SNe Ia data (Liang et al. 2010; Liang et al. 2011; Wei 2010; Wang et al. 2016; Liu et al. 2022b).

On the other side, the observational Hubble data (OHD) using the cosmic chronometers (CC) method from the galactic age differential

method (Jimenez and Loeb 2002) has advantages in constraining cosmological parameters and distinguishing DE models. This method allows for Hubble information to be directly derived from observations up to approximately $z \lesssim 2$ (Moresco et al. 2022). Amati et al. (2019) proposed an alternative method to calibrate 193 GRBs (spectral parameters taken from Demianski et al. (2017) and references therein) with firmly measured redshift by using the OHD with the CC method. Li et al. (2023) calibrated GRBs from the latest OHD using Gaussian Process to construct the GRB Hubble diagram. Xie et al. (2023) obtain a larger Ω_M values in the Λ CDM model with GRBs at high redshift, but adding OHD at low redshift removes this trend. Jia et al. (2023) indicate that H_0 value is consistent with that measured from the local data at low redshift and drops to the value measured from the CMB at high redshift with SN Ia, OHD and BAO data.

Recently, Hernández-Almada et al. (2020) constrained the PEDE and GEDE models with the latest OHD, including non-homogeneous, homogeneous and differential age Hubble data, to obtain values for the deceleration-acceleration transition redshift within a 2σ confidence level. More recently, Liang et al. (2022) used a Gaussian Process to calibrate the A118 GRB sample from the Pantheon sample and constrained DE models with GRBs at high redshift and OHD. In this work, we use the cosmology-independent GRBs in Ref. (Liang et al. 2022) at $1.4 < z \leq 8.2$ and the latest OHD obtained with the CC method which summarized in Ref. (Li et al. 2023) at $0.07 < z < 1.965$ to study the two emergent DE models: PEDE and GEDE. We use the information criterion DIC to compare the dark energy models.

The paper is organized as follows: In Section. 2, we summarize the cosmological models to be analyzed. In Section. 3, we briefly describe the observational data sets we used in this work and the corresponding analysis method. The results are shown in Section. 4. Finally, the conclusions are given in Section. 5.

2 Cosmological models

Considering a spatially flat, homogeneous, and isotropic universe and the Friedmann-Lemaître-Robertson-Walker (FLRW) metric, the Friedmann

equation can describe the evolution of the Universe with negligible radiation, pressureless matter, and DE:

$$E(a) = \left[\Omega_{m,0} \times a^{-3} + \tilde{\Omega}_{DE}(a) \right]^{-\frac{1}{2}}, \quad (1)$$

where the scale factor $a = 1/(1+z)$, $\Omega_{m,0}$ is the current density of matter at redshift $z = 0$. $\tilde{\Omega}_{DE}(a)$ is the energy density of the dark energy fluid with respect to the critical energy density at present, with $\rho_{crit,0} = 3H_0^2/8\pi G$ and $\rho_{crit}(a) = 3H^2(a)/8\pi G$. The present values of the density parameters for pressureless matter are defined as $\Omega_{m,0} = \rho_{m,0}/\rho_{crit,0}$. $\tilde{\Omega}_{DE}$ is the density of dark energy, which is defined as:

$$\begin{aligned} \tilde{\Omega}_{DE}(a) &= \frac{\rho_{DE}(a)}{\rho_{crit,0}} \\ &= \frac{\rho_{DE}(a)}{\rho_{crit}(a)} \times \frac{\rho_{crit}(a)}{\rho_{crit,0}} = \Omega_{DE,0}(a) \times \frac{H^2(a)}{H_0^2}, \end{aligned} \quad (2)$$

where $\Omega_{DE,0}$ is the current density of DE at redshift $z = 0$. Alternatively, this equation can be expressed as a function of redshift z :

$$\tilde{\Omega}_{DE}(z) = \Omega_{DE,0} \times \exp \left\{ \int_0^z \frac{1+w(z')}{1+z'} dz' \right\}, \quad (3)$$

The PEDE model (Li and Shafieloo 2019) has been proposed as a potential alternative to the Λ CDM model without additional degrees of freedom. The DE density at redshift z is given by:

$$\tilde{\Omega}_{DE}(z) = \Omega_{DE,0} \times [1 - \tanh(\log_{10}(1+z))]. \quad (4)$$

By assuming a more generalized form of EDE model including extra parameters, the DE density in the GEDE model (Li and Shafieloo 2020) is given by:

$$\tilde{\Omega}_{DE}(z) = \Omega_{DE,0} \times \frac{1 - \tanh \left(\Delta \times \log_{10} \left(\frac{1+z}{1+z_t} \right) \right)}{1 + \tanh(\Delta \times \log_{10}(1+z_t))}, \quad (5)$$

where z_t is the transition redshift, which can be derived from $\tilde{\Omega}_{DE}(z_t) = \Omega_{m,0}(1+z_t)^3$. In the GEDE model, setting $\Delta = 0$ recovers the Λ CDM model, while setting $\Delta = 1$ yields the PEDE model, with the exception that the authors (Li and Shafieloo 2020) set $z_t = 0$ for simplicity.

In this work, we also consider the Λ CDM model, the w CDM model and the Chevallier-Polarski-Linder (CPL) parameterization to consider a DE component that depends on redshift (Chevallier and Polarski 2001; Linder 2003, 2005; Barger et al. 2006) for comparison. The EoS of all the DE models can be summarized as follows:

$$w(z) = \begin{cases} -1, & \Lambda\text{CDM} \\ w_0 + \frac{w_0 z}{1+z}, & w\text{CDM} \\ -\frac{1}{3 \ln 10} \times (1 + \tanh[\log_{10}(1+z)]) - 1, & \text{CPL} \\ -\frac{\Delta}{3 \ln 10} \times \left(1 + \tanh\left[\Delta \times \log_{10}\left(\frac{1+z}{1+z_t}\right)\right]\right) - 1, & \text{PEDE, GEDE} \end{cases} \quad (6)$$

In order to facilitate model comparison and evaluate their relative merits, several well-established statistical measures were employed. These included the Akaike Information Criterion (AIC) (Akaike 1974), the Bayesian Information Criterion (BIC) (Schwarz 1978), and the Deviance Information Criterion (DIC) (Kunz et al. 2006) - all of which have found widespread application in astrophysical research. Since the AIC and BIC criteria employ only the likelihood value at maximum numerically from the Bayesian analysis, one needs to use sufficiently long chains to ensure the accuracy of \mathcal{L}_{max} . The quantity DIC, known also as the Bayesian complexity, which focus on assessing the number of parameters that can be constrained by a particular dataset, has been introduced into astrophysics. The use of DIC can provide all the information obtained from the likelihood calls during the maximization procedure. For a quantitative comparison between our proposed in this work, we employ the DIC which is defined as (Spiegelhalter et al. 2002):

$$\text{DIC} = D(\bar{\theta}) + 2p_D = \overline{D(\theta)} + p_D \quad (7)$$

where $D(\theta) = -2\ln\mathcal{L}(\theta) + C$, C is a normalized constant depending only on the data which will vanish from any derived quantity, $p_D = \overline{D(\theta)} - D(\bar{\theta})$ is the effective number of model parameters, with the deviance of the likelihood.

3 Observational data

In this section, we describe the observational data used in our analyses for constraining cosmological parameters. For the GRBs sample, we follow the cosmology-independent approach in Liang et al. (2022) to calibrate the Amati relation with the A118 GRB sample (Khadka et al. 2021) using the

Pantheon SNe Ia sample (Scolnic et al. 2018); and use GRBs data at redshifts $1.4 < z \leq 8.2$ to constrain cosmological models¹. OHD obtained using the CC method relates the evolution of differential ages of passive galaxies at different redshifts without assuming any cosmological model (Jimenez and Loeb 2002). We utilize 32 updated OHD measurements compiled from Ref. (Li et al. 2023), covering a redshift range of $0.07 < z < 1.965$, which consists of 15 correlated measurements with the corresponding covariance matrix provided by Moresco et al. (2020), and 17 uncorrelated measurements with the latter sources from (Moresco et al. 2012; Moresco 2015; Moresco et al. 2016). The cosmology-independent 98 GRBs at $1.4 < z \leq 8.2$ and 32 OHD at $0.07 < z < 1.965$ are showed in Fig. 1.

The cosmological parameters are fitted with GRBs by minimizing the χ^2 method:

$$\chi_{\text{GRB}}^2 = \sum_{i=1}^N \left[\frac{\mu_{\text{obs}}(z_i) - \mu_{\text{th}}(z_i; p, H_0)}{\sigma_{\mu_i}} \right]^2 \quad (8)$$

where $N = 98$ represents the number of GRBs at high-redshift, μ_{obs} is the observed distance modulus and σ_{μ_i} is the uncertainty associated with the observed distance modulus, μ_{th} denotes the theoretical distance modulus which determined by the cosmological parameters p with DE models and H_0 . To constrain the dark energy models using OHD, the corresponding χ_{OHD}^2 is given by: (Zhang et al. 2024)

$$\chi_{\text{OHD}}^2 = \sum_{i=1}^{17} \left[\frac{H_{\text{obs}}(z_i) - H_{\text{th}}(z_i; p, H_0)}{\sigma_{H_i}} \right]^2 + \Delta \hat{H}^T C_H^{-1} \Delta \hat{H} \quad (9)$$

where σ_{H_i} represents the observed uncertainty of the 17 uncorrelated measurements, $\Delta \hat{H} = H_{\text{obs}}(z) - H_{\text{th}}(z; p, H_0)$ represents the difference vector between the observed data and the theoretical values for the 15 correlated measurements, and C_H^{-1} is the inverse of the covariance matrix. The combine χ^2 statistic, combining GRBs and OHD is given by:

$$\chi_{\text{com}}^2 = \chi_{\text{GRB}}^2 + \chi_{\text{OHD}}^2 \quad (10)$$

¹It should be noted that the calibration results can be affected by the treatment of absolute magnitude M . We find that the calibration parameters with the A118 GRB data set are almost the same with and without marginalization over M .

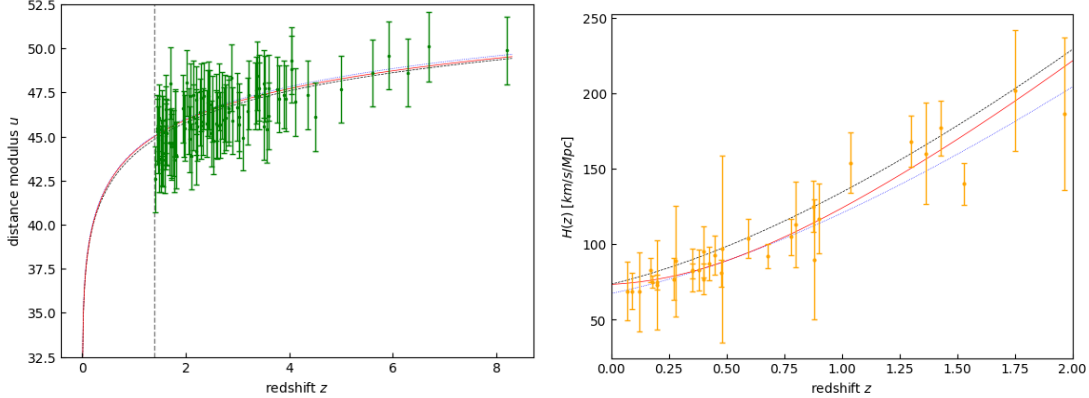


Fig. 1 The cosmology-independent 98 GRBs at $1.4 < z \leq 8.2$ (*left*) and 32 OHD at $0.07 < z < 1.965$ (*right*). The red solid curve present the predicted values from the best values of GEDE model with GRBs and OHD. The blue dotted curve and the black dashed curve are the predicted values of distance modulus for a flat Λ CDM model from CMB and SNe Ia, respectively.

4 Results

4.1 Results from GRBs and OHD

In this section, we estimate and compare the parameters of the standard Λ CDM model, the w CDM model, the CPL, the PEDE model and the GEDE model using cosmological observation data from GRBs and OHD. Through the minimization of the χ^2 value, we can obtain the best-fit parameter estimates. We employ the *emcee* Python module (Foreman-Mackey et al. 2013) in the *lmfit* python library (Newville et al. 2021). Furthermore, we utilize the GETDIST package (Lewis 2019) to analyze the sampled chains.

The results of cosmological parameters with 1σ uncertainties constraint with GRBs-only, OHD-only and GRBs + OHD for five DE models are provided in Table 1. For the case with GRBs-only, we obtain H_0 and Ω_m with the large error bars which indicate that the cosmological parameters are not well-constrained with this datasets; the Λ CDM model ($w_0 = -1$, $w_a = 0$) are consistent with the inferred value of $w_0 = -0.98 \pm 0.55$ for the w CDM model and $w_0 = -1.03^{+0.42}_{-0.83}$, $w_a = -0.20^{+1.30}_{-2.30}$ for the CPL model within 1σ uncertainty. For the case with OHD-only, we find that the value of H_0 for the PEDE model ($H_0 = 69.9 \pm 4.2 \text{ km s}^{-1} \text{ Mpc}^{-1}$) is lower than that of the GEDE model ($H_0 = 72.4 \pm 4.8 \text{ km s}^{-1} \text{ Mpc}^{-1}$), which shows agreement with the SH0ES measurement (Riess et al. 2022a,b). For the case with GRBs + OHD, the measured

H_0 ranges from $69.9 \pm 4.0 \text{ km s}^{-1} \text{ Mpc}^{-1}$ (Λ CDM) to $73.4 \pm 4.7 \text{ km s}^{-1} \text{ Mpc}^{-1}$ (GEDE). When the OHD is combined with GRBs, we find the constraints results on H_0 and Ω_m can be significantly improved and the mean values shifts in the same direction, though the overall effect is not very large. From Table 1, we can see that for all models, the constraints on H_0 and Ω_m from OHD and GRBs + OHD are well consistent with each other at 1σ CL, but in agreement with the constraint from GRBs at about 2σ . Interestingly, the constraints for the w CDM model and CPL model are not well-constrained and exhibit results distinct from the other models.

The statistical measures of the model comparison for the three datasets are also presented in Table 1. The PEDE model outperforms the Λ CDM model in both the GRBs-only and OHD-only datasets, with $\Delta\text{DIC} = -0.195$ and $\Delta\text{DIC} = -0.064$, respectively. This trend continues in the combined GRBs + OHD dataset, where the PEDE model surpasses not only the Λ CDM model but also the w CDM and CPL models across all evaluation measures. However, the GEDE model does not exhibit clear evidence of superiority over the Λ CDM, w CDM and CPL models in any of the datasets. It is noteworthy that this analysis is conducted without assuming any hard-cut prior on the Hubble constant (H_0), ensuring an unbiased comparison of the models. In summary, the PEDE model consistently demonstrates a better fit to the data compared to the Λ CDM model, as evidenced by its lower DIC values. In contrast, the w CDM

Table 1 Constraints at 68% confidence-level errors on the cosmological parameters for the different tested dark energy models with GRBs-only, OHD-only and GRBs + OHD. And at 95% confidence-level errors on the Δ for GEDE.

Parameters	H_0	Ω_m	w_0	w_a	Δ	z_t^*	χ_{md}^2	Δ DIC
GRBs-only								
Λ CDM	$72.0^{+10.0}_{-20.0}$	$0.50^{+0.18}_{-0.36}$	-	-	0	$0.060^{+0.370}_{-0.500}$	26.831	0
w CDM	$70.0^{+8.0}_{-20.0}$	$0.50^{+0.24}_{-0.36}$	-0.98 ± 0.55	-	-	$-0.120^{+0.570}_{-0.490}$	26.951	+0.368
CPL	$69.0^{+9.0}_{-20.0}$	$0.53^{+0.39}_{-0.34}$	$-1.03^{+0.42}_{-0.83}$	$-0.20^{+1.30}_{-2.30}$	-	$-0.110^{+0.580}_{-0.360}$	26.954	+0.625
PEDE	$73.0^{+10.0}_{-20.0}$	$0.52^{+0.22}_{-0.36}$	-	-	1	0.020 ± 0.360	26.884	-0.195
GEDE	$73.0^{+10.0}_{-20.0}$	$0.55^{+0.20}_{-0.31}$	-	-	$4.9 \pm 2.9^{(+4.8)}_{(-4.6)}$	$-0.001^{+0.220}_{-0.250}$	26.942	+0.204
OHD-only								
Λ CDM	68.8 ± 4.1	$0.324^{+0.048}_{-0.074}$	-	-	0	0.290 ± 0.120	14.526	0
w CDM	$70.2^{+5.6}_{-6.7}$	$0.294^{+0.084}_{-0.060}$	$-1.15^{+0.46}_{-0.57}$	-	-	$0.220^{+0.180}_{-0.140}$	15.080	+0.043
CPL	$70.5^{+5.7}_{-6.8}$	$0.305^{+0.100}_{-0.072}$	$-1.17^{+0.40}_{-0.66}$	$-0.30^{+1.30}_{-2.20}$	-	$0.270^{+0.140}_{-0.200}$	15.160	+0.322
PEDE	69.9 ± 4.2	$0.332^{+0.046}_{-0.068}$	-	-	1	0.235 ± 0.099	14.497	-0.064
GEDE	72.4 ± 4.8	$0.334^{+0.038}_{-0.063}$	-	-	$3.7^{+1.4}_{-3.5}^{(+5.4)}_{(-3.8)}$	$0.185^{+0.062}_{-0.092}$	14.752	+0.589
GRBs + OHD								
Λ CDM	69.9 ± 4.0	$0.325^{+0.049}_{-0.070}$	-	-	0	0.290 ± 0.120	43.250	0
w CDM	$71.2^{+5.2}_{-6.2}$	$0.298^{+0.081}_{-0.057}$	$-1.14^{+0.53}_{-0.43}$	-	-	$0.220^{+0.170}_{-0.140}$	43.682	+0.034
CPL	71.9 ± 6.1	$0.311^{+0.092}_{-0.067}$	$-1.18^{+0.37}_{-0.67}$	$-0.40^{+1.20}_{-2.30}$	-	$0.265^{+0.094}_{-0.190}$	43.609	+0.409
PEDE	71.0 ± 4.1	$0.335^{+0.045}_{-0.066}$	-	-	1	0.231 ± 0.095	43.221	-0.190
GEDE	73.4 ± 4.7	$0.335^{+0.040}_{-0.057}$	-	-	$3.6^{+1.3}_{-3.4}^{(+5.1)}_{(-3.7)}$	$0.184^{+0.059}_{-0.089}$	43.499	+0.606

and CPL parameterization models perform poorly in terms of DIC when compared to the Λ CDM model, highlighting the PEDE model's superiority in describing the observations across all three datasets.

In Fig. 2, we show the constrained results of the cosmological parameters for the Λ CDM and GEDE model with GRBs-only, OHD-only and GRBs + OHD datasets. We find the constraints on H_0 are all in agreement with each other at 1σ confidence level and also agree with the local results from the SH0ES collaboration (Riess et al. 2019). For the free parameter of the GEDE model, we can find that the results with GEDE exclude PEDE and Λ CDM in 1σ and with large error for GRBs-only case. $\Delta = 0$ is in agreement at about 1.7σ , and $\Delta = 1$ is at about 1.3σ . For OHD-only and GRBs + OHD datasets, we get the result with tight error bars and that PEDE is preferred, namely, Δ close to 1. We get $\Delta = 1$ is in agreement at about 1.9σ , $\Delta = 0$ is at about 2.6σ for OHD-only and $\Delta = 1$ is in agreement at about 2σ , $\Delta = 0$ is at about 2.8σ for GRBs + OHD. Λ CDM are excluded in 2σ . Interestingly, the derived parameter z_t of the GEDE model ($z_t = 0.185^{+0.062}_{-0.092}$) with OHD-only and ($z_t = 0.184^{+0.059}_{-0.089}$) with GRBs + OHD are in agreement with the result of Hernández-Almada et al.

($z_t = 0.174^{+0.083}_{-0.064}$) from OHD sample (Hernández-Almada et al. 2020). Our result are also consistent with Liu et al. (2022a).

In Fig. 3, we present the constraints on H_0 and Ω_m for the Λ CDM, w CDM, CPL, PEDE and GEDE models using the combined OHD and GRBs. We can find that the PEDE and GEDE models yield higher values with a clear trend for both parameters of H_0 and Ω_m compared to Λ CDM. Furthermore, the GEDE model exhibits even more higher values than the PEDE model. These findings suggest that the EDE models have the potential to alleviate the H_0 tension. It is evident that the PEDE model and GEDE model can yield a higher best-fit value of H_0 than the Λ CDM model when considering the GRBs-only, OHD-only and GRBs + OHD cases. These results are more consistent with those from the SH0ES collaboration (Riess et al. 2019).

In Fig. 4, we show the evolution of dark energy density $\Omega_{DE}(z)$ as a function of redshift z . We can see an emergent dark energy behavior from GRBs + OHD data, and the cosmological constant is outside the 2σ confidence limits.

We find our results are compatible with the previous works of Li et al. (Li and Shafieloo 2019, 2020), where the authors observed that the value of H_0 derived from the Λ CDM and CPL parameterization models is close to the CMB prediction,

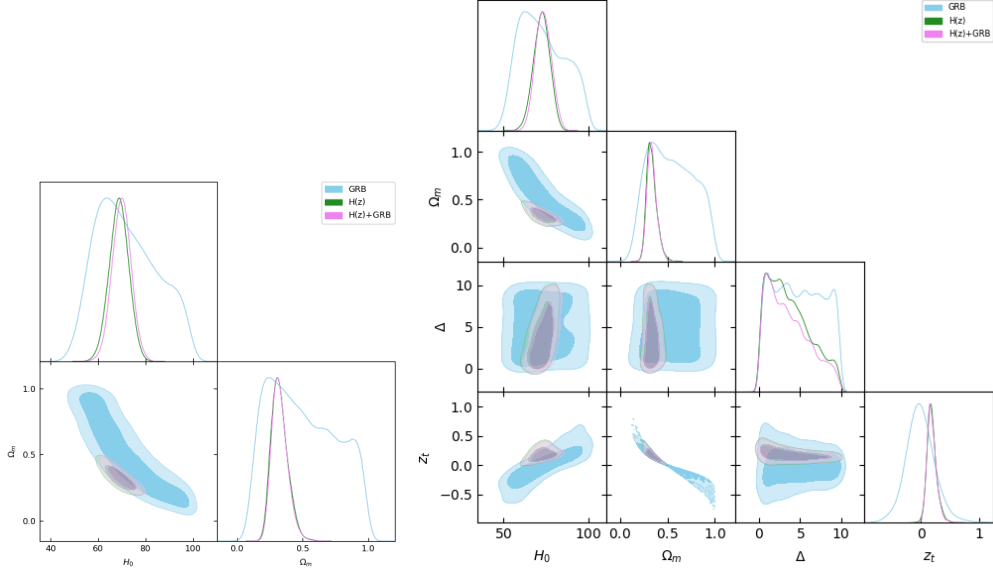


Fig. 2 Contours with 1σ and 2σ CL of cosmological parameters (H_0 and Ω_m) for the Λ CDM model (*left*) and cosmological parameters (H_0 , Ω_m and Δ) in the framework of GEDE (*right*) from GRBs-only, OHD-only, GRBs + OHD. Note that z_t is not a free parameter and is shown for clarity.

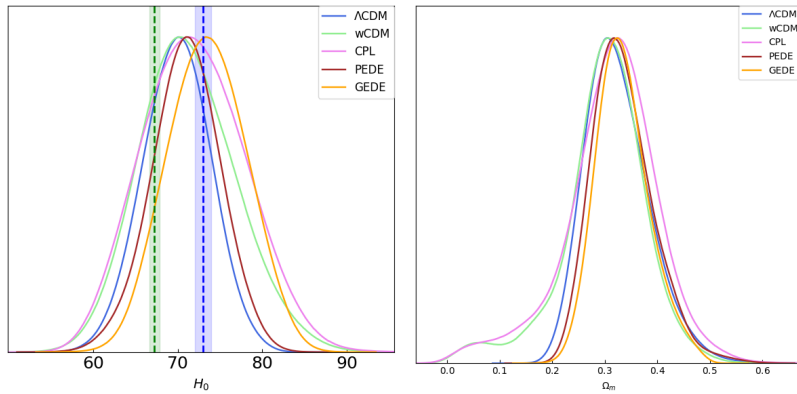


Fig. 3 The constraints for H_0 (*left*) and Ω_m (*right*) with the Λ CDM, w CDM, CPL, PEDE and GEDE model from the GRBs + OHD data. The blue line, green line and violet line represent the result from Λ CDM, w CDM and CPL. The brown and orange lines represent the result from PEDE and GEDE respectively. The blue shadows show the H_0 results with 1σ uncertainty from Riess et al. (Riess et al. 2019), the green shadows show the H_0 results with 1σ uncertainty from Planck CMB observations (Planck Collaboration et al. 2020).

regardless of whether the dataset includes CMB data or not. The authors also found that the value of H_0 aligns closely with the local measurement value obtained by the SH0ES collaboration when assuming 1σ and 2σ priors for H_0 taken from the SH0ES result. Our result is compatible with their findings, but it is important to emphasize that we perform our analysis without assuming any hard-cut prior on H_0 .

4.2 Results from GRBs, OHD and BAOs

BAOs serve as a universal standard ruler evolving with the Universe, offering a distinct perspective on the universe's structure and evolution, which can be used as an invaluable tool for probing cosmological models (Rezaei et al. 2020; Shah et al. 2023; Rezaei et al. 2022; Staicova

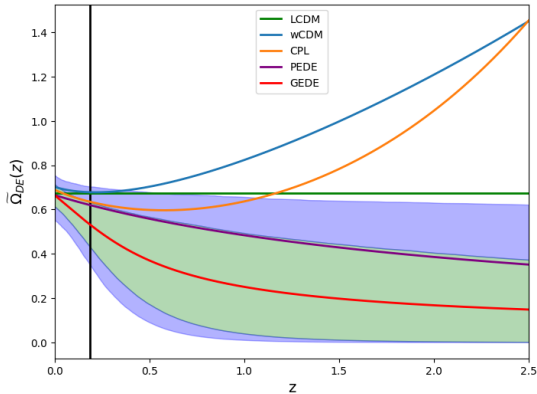


Fig. 4 The evolution of dark energy density $\tilde{\Omega}_{DE}(z)$ from $z = 0$ to 2.5. The green and dark blue regions are the 1σ and 2σ confidence ranges of the GEDE model fitting GRBs + OHD data. The green, blue, orange, purple and red solid lines are the best-fit results from the Λ CDM, w CDM, CPL, PEDE and GEDE models, respectively. The vertical lines display the mean values of z_t from GRBs + OHD.

and Benisty 2022). In order to refine our analysis and tighten the constraints on cosmological parameters, we combine mid-redshift observations GRBs and OHD with BAOs. It should be noted that BAO measurements which under a fiducial cosmology could provide biased constraints (Hernández-Almada et al. 2020). Here we use the 6dF Galaxy Survey (6dFGS) at $z_{\text{eff}} = 0.106$ (Beutler et al. 2011), the Sloan Digital Sky Survey (SDSS) DR7 Main Galaxy Sample (MGS) at $z_{\text{eff}} = 0.15$ (Ross et al. 2015), and nine measurements from the extended Baryon Oscillation Spectroscopic Survey (eBOSS) DR16 at $z_{\text{eff}} = 0.38, 0.51, 0.70, 0.85, 1.48$ (Alam et al. 2021). The likelihood of BAO for different datasets can be expressed as,

$$\chi_{\text{BAO}}^2 = \Delta P_{\text{BAO}} C_{\text{BAO}}^{-1} \Delta P_{\text{BAO}}^T, \quad (11)$$

where C_{BAO} is the covariance matrix², $\Delta P_{\text{BAO}} = v_{\text{obs}}(z) - v_{\text{th}}(z)$, $v_{\text{obs}}(z)$ is a BAO measurement of the observed points at each z , and $v_{\text{th}}(z)$ is the prediction of the theoretical model. The BAO feature appears in both the line-of-sight direction and the transverse direction and provides measurements of the radial projection D_H and the transverse comoving distance $D_M(z)$ with $\frac{D_H(z)}{r_d} =$

²For uncorrelated points the covariance matrix is a diagonal matrix, and its elements are the inverse errors, and for correlated points, the covariance matrices are from (Alam et al. 2021).

$\frac{c}{H(z)r_d}$ and $\frac{D_M(z)}{r_d} = \frac{c}{H_0 r_d} \Gamma(z)$, where r_d is the sound horizon at the drag epoch $r_s(z_d)$ ³, and $\Gamma(z) = \int_0^z dz' / E(z')$. The angular diameter distance $D_A(z)$ has relation with $D_M(z)$: $D_A(z) = D_M(z)/(1+z)$. The total χ^2 statistic, combining GRBs, OHD and BAOs, is given by:

$$\chi_{\text{tot}}^2 = \chi_{\text{GRB}}^2 + \chi_{\text{OHD}}^2 + \chi_{\text{BAO}}^2. \quad (12)$$

Results from GRBs, OHD and BAOs for DE models are summerizd in Table 2. It should be noted that Rezaei et al. applied the statistical Bayesian evidence with the combining observational datasets by to indicate that the PEDE models are not favored (Rezaei et al. 2020); Shah et al. (2023) used the latest datasets of SNIa, CMB, and BAOs to conclude that the PEDE model cannot resolve the tension with the SH0ES measurement within 1σ . We find a significant improvement in the precision of cosmological parameter estimations, evidenced by a marked decrease in the width of the error bars, when adding BAO data into the joint analysis. Our results indicate that PEDE model is still a favorite model from GRBs, OHD and BAOs. The statistical limit in our results from GRBs, OHD and BAOs can alleviated the tension with the SH0ES measurement by 0.81σ . We obtain H_0 of $67.8 \pm 2.5 \text{ km s}^{-1} \text{ Mpc}^{-1}$, and $\Omega_m = 0.358_{-0.040}^{+0.034}$ for the Λ CDM model, and the two EDE models perform well our analysis with GRBs, OHD, and BAOs. These results are in consistent with those in (Staicova and Benisty 2022) for the Λ CDM model and EDE models by adding SN Ia dataset and two BAO datasets.

4.3 Results from the simultaneous fitting method

Finally, we constrain the Λ CDM, PEDE and GEDE models by using the simultaneous fitting method (Amati et al. 2019), in which the parameters of DE models and the relation parameters of GRBs are fitted simultaneously. Results with the data combination are shown in Fig.

³The comoving sound horizon $r_s(z)$ is given as (Eisenstein and Hu 1998): $r_s(z) = \frac{c}{H_0} \int_z^\infty \frac{c_s}{E(z') dz'}$. The redshift of the drag epoch can be approximated as (Hu and Sugiyama 1996): $z_d = \frac{1345 \omega_m^{0.251}}{1 + 0.659 \omega_m^{0.828}} [1 + b_1 \omega_b^{b_2}]$, where $b_1 = 0.313 \omega_m^{-0.419} [1 + 0.607 \omega_m^{0.674}]$, $b_2 = 0.238 \omega_m^{0.223}$ with $\omega_b = \Omega_b h^2$ and $\omega_m = \Omega_m h^2$.

Table 2 Constraints at 68% confidence-level errors on the cosmological parameters for DE models with GRBs + OHD + BAOs. And at 95% confidence-level errors on the Δ for GEDE.

Parameters	H_0	Ω_m	w_0	w_a	Δ	z_t^*	χ_{md}^2	ΔDIC
GRBs + OHD + BAO								
ΛCDM	67.8 ± 2.5	$0.358^{+0.034}_{-0.040}$	-	-	0	0.219 ± 0.067	45.070	0
$w\text{CDM}$	$68.8^{+3.6}_{-4.3}$	$0.358^{+0.040}_{-0.049}$	$-1.13^{+0.30}_{-0.17}$	-	-	$0.203^{+0.073}_{-0.100}$	45.190	+2.275
CPL	$67.6^{+3.8}_{-4.3}$	0.375 ± 0.052	-0.85 ± 0.34	$-0.94^{+0.93}_{-1.70}$	-	0.203 ± 0.079	44.953	+2.183
PEDE	70.6 ± 2.8	$0.346^{+0.034}_{-0.041}$	-	-	1	0.208 ± 0.059	45.494	+0.489
GEDE	$70.4^{+3.0}_{-3.4}$	$0.345^{+0.034}_{-0.041}$	-	-	$1.02^{+0.41}_{-1.00} (^{+1.60}_{-1.00})$	0.210 ± 0.061	45.282	+1.178

5. For the ΛCDM model, we obtain: $H_0 = 70.7^{+1.8}_{-2.0} \text{ km s}^{-1} \text{ Mpc}^{-1}$ and $\Omega_m = 0.308 \pm 0.017$, which are consistent with the results by Liang et al. (2022). For PEDE model and GEDE model, $H_0 = 74.2 \pm 1.9 \text{ km s}^{-1} \text{ Mpc}^{-1}$ for the PEDE model and $H_0 = 72.3^{+2.0}_{-2.4} \text{ km s}^{-1} \text{ Mpc}^{-1}$ for the GEDE model, respectively. Both EDE models yield similar results for the relation parameters, which are close to the local measurement with the SH0ES measurement.

5 Conclusions

In this work, we have investigated the viability of the PEDE and the GEDE models with cosmology-independent observational data including GRBs and OHD samples. The joint datasets of GRBs + OHD in the mid-redshift region between the local the distance ladder SN Ia and CMB appear to provide much better constraints on the DE parameters and the value of H_0 . For comparison, we also consider the ΛCDM model, the $w\text{CDM}$ model and the CPL model. With a Bayesian statistical approach for parameter inference and model selection, we find that PEDE and GEDE derive higher H_0 compare to ΛCDM , which support the viability of EDE models as a description of DE behavior and provide new evidence for their potential as an important supplement and possible alternative to the ΛCDM model. Our results indicate that EDE models are at least competitive with the ΛCDM model in describing the accelerated expansion of the universe and can alleviate the H_0 tension problem, which are consistent with previous analyses (Li and Shafieloo 2019, 2020; Pan et al. 2020; Hernández-Almada et al. 2020; Liu et al. 2022a).

In conclusion, our work demonstrates that the EDE models can better represent the effective behavior of DE compared to the ΛCDM model and can reduce tensions in the estimation of H_0 .

Given the challenges faced by the standard cosmological model, this implies that EDE models can be competitive cosmological models. Future theoretical explorations and observational verifications are needed to further test the validity of EDE models. Recently, it should be note that the potential use of machine learning (ML) algorithms for cosmological use with GRBs (Luongo and Muccino 2021; Zhang et al. 2023; Shah et al. 2024) and OHD (Bengaly et al. 2023; Gangopadhyay et al. 2023). Moreover, the running of H_0 evolving with redshift is an interesting idea for the H_0 tension (Dainotti et al. 2021; Ó Colgáin et al. 2022; Jia et al. 2023; Hu and Wang 2023). Hu et al. (2024) tested the cosmological principle by the region fitting (RF) method with Pantheon+ sample to simultaneously map matter-density distribution and the Hubble expansion distribution. The results provide clear indications for a possible cosmic anisotropy. Only with support from multiple lines of evidence can we ultimately determine the status of EDE models in explaining the H_0 tension.

ACKNOWLEDGMENTS

We thank HuiFeng Wang, Xiaodong Nong, Zhen Huang and Xin Luo for discussions. We are also grateful to the reviewers for their comments and suggestions.

Funding This project was supported by the Guizhou Provincail Science and Technology Foundation: QKHJC-ZK[2021] Key 020 and QKHJC-ZK[2024] general 443. X. Li was supported by NSFC No. 12003006, Science Research Project of Hebei Education Department No. BJK2024134 and the fund of Hebei Normal University No. L2020B02.

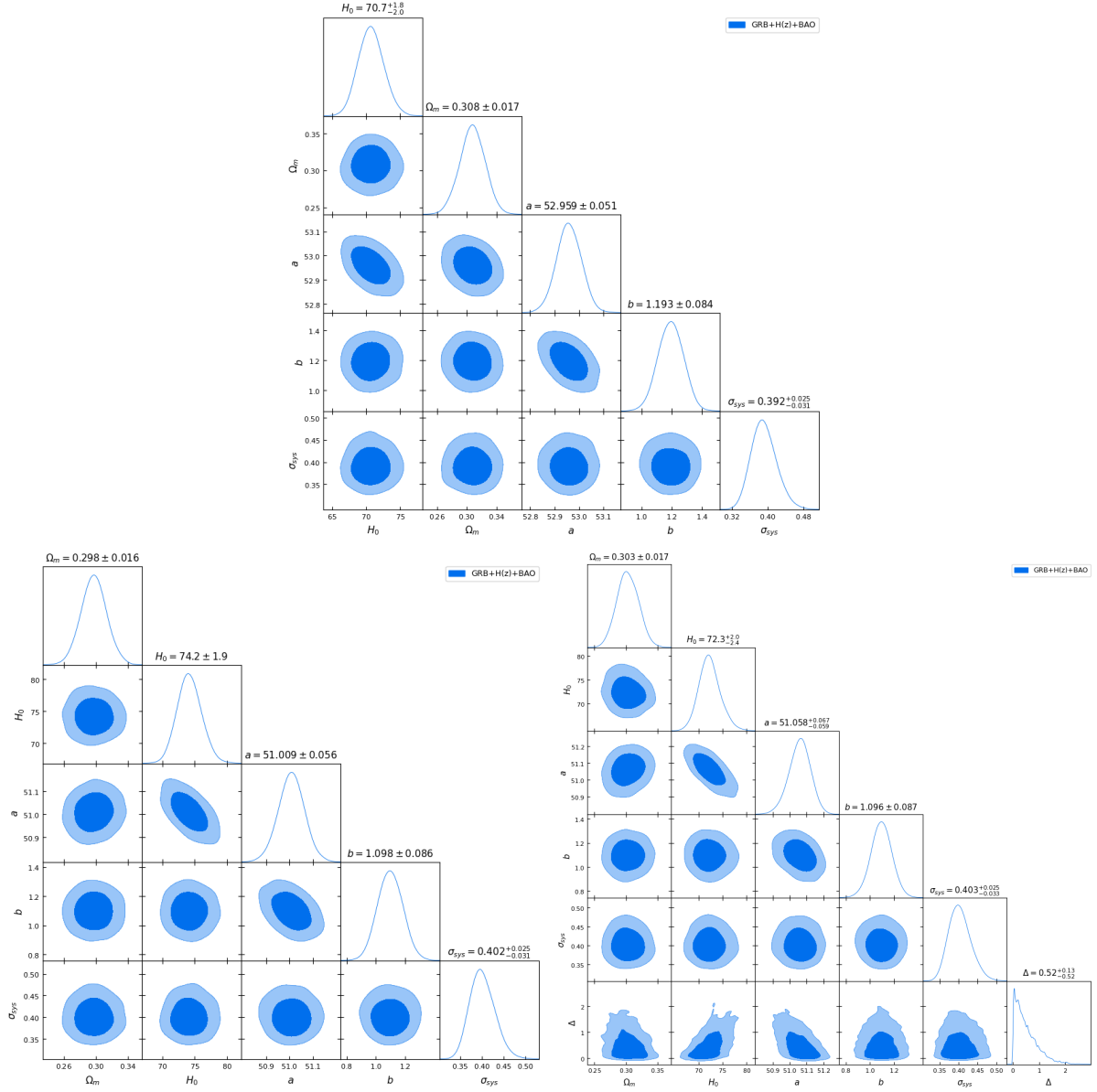


Fig. 5 Simultaneous fitting of cosmological parameters (Ω_m, H_0) and GRB calibration parameters (a, b, σ_{sys}) with GRBs + OHD + BAO. The top panel is the Λ CDM, the bottom left is the PEDE, the bottom right is the GEDE model.

Data Availability No datasets were generated or analysed during the current study.

Declarations

Competing interests The authors declare no competing interests.

Ethics approval Not applicable.

References

- Akaike H (1974) A new look at the statistical model identification. *IEEE Transactions on Automatic Control* 19(6):716. <https://doi.org/10.1109/TAC.1974.1100705>
- Alam S, Aubert M, Avila S, et al. (2021) Completed SDSS-IV extended Baryon Oscillation

- Spectroscopic Survey: Cosmological implications from two decades of spectroscopic surveys at the Apache Point Observatory. *Physical Review D* 103(8):083533. <https://doi.org/10.1103/PhysRevD.103.083533> [astro-ph.CO]
- Alam U, Bag S, Sahni V (2017) Constraining the cosmology of the phantom brane using distance measures. *Physical Review D* 95(2):023524. <https://doi.org/10.1103/PhysRevD.95.023524>
- Amati L, D'Agostino R, Luongo O, et al. (2019) Addressing the circularity problem in the E_p - E_{iso} correlation of gamma-ray bursts. *Monthly Notices of the Royal Astronomical Society: Letters* 486(1):L46. <https://doi.org/10.1093/mnrasl/slz056>
- Barger V, Guarnaccia E, Marfatia D (2006) Classification of dark energy models in the (w_0, w_a) plane. *Physics Letters B* 635(2-3):61. <https://doi.org/10.1016/j.physletb.2006.02.018>
- Bengaly C, Aldinez Dantas M, Casarini L, et al. (2023) Measuring the Hubble constant with cosmic chronometers: a machine learning approach. *European Physical Journal C* 83(6):548. <https://doi.org/10.1140/epjc/s10052-023-11734-1> [astro-ph.CO]
- Beutler F, Blake C, Colless M, et al. (2011) The 6dF Galaxy Survey: baryon acoustic oscillations and the local Hubble constant. *Monthly Notices of the Royal Astronomical Society* 416(4):3017. <https://doi.org/10.1111/j.1365-2966.2011.19250.x>
- Bunn EF (2007) Systematic errors in cosmic microwave background interferometry. *Physical Review D* 75(8):083517. <https://doi.org/10.1103/PhysRevD.75.083517> [astro-ph]
- Chevallier M, Polarski D (2001) Accelerating Universes with Scaling Dark Matter. *International Journal of Modern Physics D* 10(2):213. <https://doi.org/10.1142/S0218271801000822>
- Cucchiara A, Levan AJ, Fox DB, et al. (2011) A Photometric Redshift of $z \sim 9.4$ for GRB 090429B. *The Astrophysical Journal* 736(1):7. <https://doi.org/10.1088/0004-637X/736/1/7>
- Dai ZG, Liang EW, Xu D (2004) Constraining Ω_M and Dark Energy with Gamma-Ray Bursts. *The Astrophysical Journal Letters* 612(2):L101. <https://doi.org/10.1086/424694>
- Dainotti MG, De Simone B, Schiavone T, et al. (2021) On the Hubble Constant Tension in the SNe Ia Pantheon Sample. *The Astrophysical Journal* 912(2):150. <https://doi.org/10.3847/1538-4357/abeb73>
- Demianski M, Piedipalumbo E, Sawant D, et al. (2017) Cosmology with gamma-ray bursts. I. The Hubble diagram through the calibrated $E_{p,i}$ - E_{iso} correlation. *Astronomy & Astrophysics* 598:A112. <https://doi.org/10.1051/0004-6361/201628909>
- Di Valentino E, Mena O, Pan S, et al. (2021) In the realm of the Hubble tension—a review of solutions. *Classical and Quantum Gravity* 38(15):153001. <https://doi.org/10.1088/1361-6382/ac086d> [astro-ph.CO]
- Eisenstein DJ, Hu W (1998) Baryonic Features in the Matter Transfer Function. *The Astrophysical Journal* 496(2):605. <https://doi.org/10.1086/305424> [astro-ph]
- Foreman-Mackey D, Hogg DW, Lang D, et al. (2013) emcee: The MCMC Hammer. *Publications of the Astronomical Society of the Pacific* 125(925):306. <https://doi.org/10.1086/670067>
- Freedman WL, Madore BF (2010) The Hubble Constant. *Annual Review of Astronomy and Astrophysics* 48:673. <https://doi.org/10.1146/annurev-astro-082708-101829>
- Gangopadhyay MR, Sami M, Sharma MK (2023) Phantom dark energy as a natural selection of evolutionary processes a la genetic algorithm and cosmological tensions. *Physical Review D* 108(10):103526. <https://doi.org/10.1103/PhysRevD.108.103526> [astro-ph.CO]
- Ghirlanda G, Ghisellini G, Firmani C (2006) Gamma-ray bursts as standard candles to constrain the cosmological parameters. *New Journal of Physics* 8(7):123. <https://doi.org/10.1088/1367-2630/8/7/123>

- Hernández-Almada A, Leon G, Magaña J, et al. (2020) Generalized emergent dark energy: observational Hubble data constraints and stability analysis. *Monthly Notices of the Royal Astronomical Society* 497(2):1590. <https://doi.org/10.1093/mnras/staa2052>
- Hu JP, Wang FY (2023) Hubble Tension: The Evidence of New Physics. *Universe* 9(2):94. <https://doi.org/10.3390/universe9020094> [astro-ph.CO]
- Hu JP, Wang YY, Hu J, et al. (2024) Testing the cosmological principle with the Pantheon+ sample and the region-fitting method. *Astronomy & Astrophysics* 681:A88. <https://doi.org/10.1051/0004-6361/202347121> [astro-ph.CO]
- Hu W, Sugiyama N (1996) Small-Scale Cosmological Perturbations: an Analytic Approach. *The Astrophysical Journal* 471:542. <https://doi.org/10.1086/177989> [astro-ph]
- Ichiki K, Nagata R (2009) Brute force reconstruction of the primordial fluctuation spectrum from five-year Wilkinson Microwave Anisotropy Probe observations. *Physical Review D* 80(8):083002. <https://doi.org/10.1103/PhysRevD.80.083002>
- Jia XD, Hu JP, Wang FY (2023) Evidence of a decreasing trend for the Hubble constant. *Astronomy & Astrophysics* 674:A45. <https://doi.org/10.1051/0004-6361/202346356>
- Jimenez R, Loeb A (2002) Constraining Cosmological Parameters Based on Relative Galaxy Ages. *The Astrophysical Journal* 573(1):37. <https://doi.org/10.1086/340549>
- Khadka N, Luongo O, Muccino M, et al. (2021) Do gamma-ray burst measurements provide a useful test of cosmological models? *Journal of Cosmology and Astroparticle Physics* 2021(9):042. <https://doi.org/10.1088/1475-7516/2021/09/042>
- Komatsu E, Smith KM, Dunkley J, et al. (2011) Seven-year Wilkinson Microwave Anisotropy Probe (WMAP) Observations: Cosmological Interpretation. *The Astrophysical Journal Supplement Series* 192(2):18. <https://doi.org/10.1088/0067-0049/192/2/18>
- Koo H, Shafieloo A, Keeley RE, et al. (2020) Model-independent Constraints on Type Ia Supernova Light-curve Hyperparameters and Reconstructions of the Expansion History of the Universe. *The Astrophysical Journal* 899(1):9. <https://doi.org/10.3847/1538-4357/ab9c9a>
- Kunz M, Trotta R, Parkinson DR (2006) Measuring the effective complexity of cosmological models. *Physical Review D* 74(2):023503
- Lewis A (2019) GetDist: a Python package for analysing Monte Carlo samples. arXiv e-prints arXiv:1910.13970. <https://doi.org/10.48550/arXiv.1910.13970>
- Li X, Shafieloo A (2019) A simple phenomenological emergent dark energy model can resolve the hubble tension. *The Astrophysical Journal* 883(1):L3. <https://doi.org/10.3847/2041-8213/ab3e09>
- Li X, Shafieloo A (2020) Evidence for emergent dark energy. *The Astrophysical Journal* 902(1):58. <https://doi.org/10.3847/1538-4357/abb3d0>
- Li Z, Zhang B, Liang N (2023) Testing dark energy models with gamma-ray bursts calibrated from the observational H(z) data through a Gaussian process. *Monthly Notices of the Royal Astronomical Society* 521(3):4406. <https://doi.org/10.1093/mnras/stad838>
- Liang N, Xiao WK, Liu Y, et al. (2008) A Cosmology-Independent Calibration of Gamma-Ray Burst Luminosity Relations and the Hubble Diagram. *The Astrophysical Journal Letters* 685(1):354. <https://doi.org/10.1086/590903>
- Liang N, Wu P, Zhang SN (2010) Constraints on cosmological models and reconstructing the acceleration history of the universe with gamma-ray burst distance indicators. *Physical Review D* 81(8):083518. <https://doi.org/10.1103/PhysRevD.81.083518>
- Liang N, Xu L, Zhu ZH (2011) Constraints on the generalized Chaplygin gas model

- including gamma-ray bursts via a Markov Chain Monte Carlo approach. *Astronomy & Astrophysics* 527:A11. <https://doi.org/10.1051/0004-6361/201015919>
- Liang N, Li Z, Xie X, et al. (2022) Calibrating Gamma-Ray Bursts by Using a Gaussian Process with Type Ia Supernovae. *The Astrophysical Journal* 941(1):84. <https://doi.org/10.3847/1538-4357/aca08a>
- Linder EV (2003) Cosmic shear with next generation redshift surveys as a cosmological probe. *Physical Review D* 68(8):083503. <https://doi.org/10.1103/PhysRevD.68.083503>
- Linder EV (2005) Cosmic growth history and expansion history. *Physical Review D* 72(4):043529. <https://doi.org/10.1103/PhysRevD.72.043529>
- Liu T, Cao S, Li X, et al. (2022a) Revising the Hubble constant, spatial curvature and dark energy dynamics with the latest observations of quasars. *Astronomy & Astrophysics* 668:A51. <https://doi.org/10.1051/0004-6361/202243375>
- Liu Y, Liang N, Xie X, et al. (2022b) Gamma-Ray Burst Constraints on Cosmological Models from the Improved Amati Correlation. *The Astrophysical Journal* 935(1):7. <https://doi.org/10.3847/1538-4357/ac7de5>
- Luongo O, Muccino M (2021) Model-independent calibrations of gamma-ray bursts using machine learning. *Monthly Notices of the Royal Astronomical Society: Letters* 503(3):4581. <https://doi.org/10.1093/mnras/stab795> [astro-ph.CO]
- Moresco M (2015) Raising the bar: new constraints on the Hubble parameter with cosmic chronometers at $z \sim 2$. *Monthly Notices of the Royal Astronomical Society: Letters* 450:L16. <https://doi.org/10.1093/mnrasl/slv037>
- Moresco M, Cimatti A, Jimenez R, et al. (2012) Improved constraints on the expansion rate of the Universe up to $z \sim 1.1$ from the spectroscopic evolution of cosmic chronometers. *Journal of Cosmology and Astroparticle Physics* 2012(8):006. <https://doi.org/10.1088/1475-7516/2012/08/006>
- Moresco M, Pozzetti L, Cimatti A, et al. (2016) A 6% measurement of the Hubble parameter at $z \sim 0.45$: direct evidence of the epoch of cosmic re-acceleration. *Journal of Cosmology and Astroparticle Physics* 2016(5):014. <https://doi.org/10.1088/1475-7516/2016/05/014>
- Moresco M, Jimenez R, Verde L, et al. (2020) Setting the Stage for Cosmic Chronometers. II. Impact of Stellar Population Synthesis Models Systematics and Full Covariance Matrix. *The Astrophysical Journal* 898(1):82. <https://doi.org/10.3847/1538-4357/ab9eb0>
- Moresco M, Amati L, Amendola L, et al. (2022) Unveiling the Universe with emerging cosmological probes. *Living Reviews in Relativity* 25(1):6. <https://doi.org/10.1007/s41114-022-00040-z>
- Motta V, García-Aspeitia MA, Hernández-Almada A, et al. (2021) Taxonomy of Dark Energy Models. *Universe* 7(6):163. <https://doi.org/10.3390/universe7060163>
- Newville M, Otten R, Nelson A, et al. (2021) lmfit/lmfit-py. <https://doi.org/10.5281/zenodo.4516644>
- Ó Colgáin E, Sheikh-Jabbari MM, Solomon R, et al. (2022) Revealing intrinsic flat Λ CDM biases with standardizable candles. *Physical Review D* 106(4):L041301. <https://doi.org/10.1103/PhysRevD.106.L041301>
- O’Dea D, Challinor A, Johnson BR (2007) Systematic errors in cosmic microwave background polarization measurements. *Monthly Notices of the Royal Astronomical Society* 376(4):1767. <https://doi.org/10.1111/j.1365-2966.2007.11558.x> [astro-ph]
- Pan S, Yang W, Di Valentino E, et al. (2020) Reconciling H_0 tension in a six parameter space? *Journal of Cosmology and Astroparticle Physics* 2020(6):062. <https://doi.org/10.1088/1475-7516/2020/06/062>
- Perlmutter S, Aldering G, Goldhaber G, et al. (1999) Measurements of Ω and Λ from 42 High-Redshift Supernovae. *The Astrophysical Journal* 517(2):565. <https://doi.org/10.1086/307221>

- Planck Collaboration, Ade PAR, Aghanim N, et al. (2016) Planck 2015 results. XIII. Cosmological parameters. *Astronomy & Astrophysics* 594:A13. <https://doi.org/10.1051/0004-6361/201525830>
- Planck Collaboration, Aghanim N, Akrami Y, et al. (2020) Planck 2018 results. VI. Cosmological parameters. *Astronomy & Astrophysics* 641:A6. <https://doi.org/10.1051/0004-6361/201833910>
- Rezaei M, Naderi T, Malekjani M, et al. (2020) A Bayesian comparison between Λ CDM and phenomenologically emergent dark energy models. *European Physical Journal C* 80(5):374. <https://doi.org/10.1140/epjc/s10052-020-7942-6> [astro-ph.CO]
- Rezaei M, Solà Peracaula J, Malekjani M (2022) Cosmographic approach to Running Vacuum dark energy models: new constraints using BAOs and Hubble diagrams at higher redshifts. *Monthly Notices of the Royal Astronomical Society* 509(2):2593. <https://doi.org/10.1093/mnras/stab3117> [astro-ph.CO]
- Riess AG, Filippenko AV, Challis P, et al. (1998) Observational Evidence from Supernovae for an Accelerating Universe and a Cosmological Constant. *The Astronomical Journal* 116(3):1009. <https://doi.org/10.1086/300499>
- Riess AG, Strolger LG, Casertano S, et al. (2007) New Hubble Space Telescope Discoveries of Type Ia Supernovae at $z \lesssim 1$: Narrowing Constraints on the Early Behavior of Dark Energy. *The Astrophysical Journal* 659(1):98. <https://doi.org/10.1086/510378>
- Riess AG, Macri LM, Hoffmann SL, et al. (2016) A 2.4% Determination of the Local Value of the Hubble Constant. *The Astrophysical Journal* 826(1):56. <https://doi.org/10.3847/0004-637X/826/1/56>
- Riess AG, Rodney SA, Scolnic DM, et al. (2018) Type Ia Supernova Distances at Redshift >1.5 from the Hubble Space Telescope Multi-cycle Treasury Programs: The Early Expansion Rate. *The Astrophysical Journal* 853(2):126. <https://doi.org/10.3847/1538-4357/aaa5a9>
- Riess AG, Casertano S, Yuan W, et al. (2019) Large Magellanic Cloud Cepheid Standards Provide a 1% Foundation for the Determination of the Hubble Constant and Stronger Evidence for Physics beyond Λ CDM. *The Astrophysical Journal* 876(1):85. <https://doi.org/10.3847/1538-4357/ab1422>
- Riess AG, Breuval L, et al. (2022a) Cluster Cepheids with High Precision Gaia Parallaxes, Low Zero-point Uncertainties, and Hubble Space Telescope Photometry. *The Astrophysical Journal* 938(1):36. <https://doi.org/10.3847/1538-4357/ac8f24>
- Riess AG, Yuan W, Macri LM, et al. (2022b) A Comprehensive Measurement of the Local Value of the Hubble Constant with $1 \text{ km s}^{-1} \text{ Mpc}^{-1}$ Uncertainty from the Hubble Space Telescope and the SH0ES Team. *The Astrophysical Journal Letters* 934(1):L7. <https://doi.org/10.3847/2041-8213/ac5c5b>
- Ross AJ, Samushia L, Howlett C, et al. (2015) The clustering of the SDSS DR7 main Galaxy sample - I. A 4 per cent distance measure at $z = 0.15$. *Monthly Notices of the Royal Astronomical Society* 449(1):835. <https://doi.org/10.1093/mnras/stv154>
- Schwarz G (1978) Estimating the dimension of a model. *The annals of statistics* p 461
- Scolnic DM, Jones DO, Rest A, et al. (2018) The Complete Light-curve Sample of Spectroscopically Confirmed SNe Ia from Pan-STARRS1 and Cosmological Constraints from the Combined Pantheon Sample. *The Astrophysical Journal* 859(2):101. <https://doi.org/10.3847/1538-4357/aab9bb>
- Shah R, Bhaumik A, Mukherjee P, et al. (2023) A thorough investigation of the prospects of eLISA in addressing the Hubble tension: Fisher forecast, MCMC and Machine Learning. *Journal of Cosmology and Astroparticle Physics* 2023(6):038. <https://doi.org/10.1088/1475-7516/2023/06/038> [astro-ph.CO]
- Shah R, Saha S, Mukherjee P, et al. (2024) LADDER: Revisiting the Cosmic Distance Ladder with Deep Learning

- Approaches and Exploring its Applications. arXiv e-prints arXiv:2401.17029. <https://doi.org/10.48550/arXiv.2401.17029> [astro-ph.CO]
- Spiegelhalter D, Best N, Carlin B (2002) Bayesian measures of model complexity and fit. *Journal of the Royal Statistical Society, Series B* 64:583
- Staicova D, Benisty D (2022) Constraining the dark energy models using baryon acoustic oscillations: An approach independent of $H_0 \cdot r_d$. *Astronomy & Astrophysics* 668:A135. <https://doi.org/10.1051/0004-6361/202244366> [astro-ph.CO]
- Tanvir NR, Fox DB, Levan AJ, et al. (2009) A γ -ray burst at a redshift of $z \sim 8.2$. *Nature* 461(7268):1254. <https://doi.org/10.1038/nature08459>
- Wang JS, Wang FY, Cheng KS, et al. (2016) Measuring dark energy with the $E_{iso} - E_p$ correlation of gamma-ray bursts using model-independent methods. *Astronomy & Astrophysics* 585:A68. <https://doi.org/10.1051/0004-6361/201526485>
- Wei H (2010) Observational constraints on cosmological models with the updated long gamma-ray bursts. *Journal of Cosmology and Astroparticle Physics* 2010(8):020. <https://doi.org/10.1088/1475-7516/2010/08/020>
- Xie H, Nong X, Zhang B, et al. (2023) Constraints on Cosmological Models with Gamma-Ray Bursts in Cosmology-Independent Way. arXiv e-prints arXiv:2307.16467. <https://doi.org/10.48550/arXiv.2307.16467>
- Yang W, Giarè W, Pan S, et al. (2023) Revealing the effects of curvature on the cosmological models. *Physical Review D* 107(6):063509. <https://doi.org/10.1103/PhysRevD.107.063509>
- Zhang B, Xie X, Nong X, et al. (2023) Model-independent Gamma-Ray Bursts Constraints on Cosmological Models Using Machine Learning. arXiv e-prints arXiv:2312.09440. <https://doi.org/10.48550/arXiv.2312.09440> [astro-ph.CO]
- Zhang H, Liu Y, Yu H, et al. (2024) Constraints on cosmological models from quasars calibrated with type Ia supernova by a Gaussian process. *Monthly Notices of the Royal Astronomical Society* 530(4):4493. <https://doi.org/10.1093/mnras/stae1120> [astro-ph.CO]
- Zhao GB, Wang Y, Saito S, et al. (2019) The clustering of the SDSS-IV extended Baryon Oscillation Spectroscopic Survey DR14 quasar sample: a tomographic measurement of cosmic structure growth and expansion rate based on optimal redshift weights. *Monthly Notices of the Royal Astronomical Society* 482(3):3497. <https://doi.org/10.1093/mnras/sty2845>